

Environmental Science Processes & Impacts

Accepted Manuscript



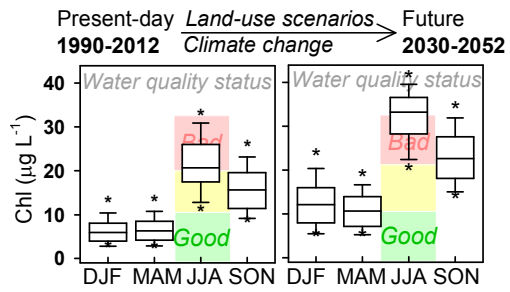
This is an *Accepted Manuscript*, which has been through the Royal Society of Chemistry peer review process and has been accepted for publication.

Accepted Manuscripts are published online shortly after acceptance, before technical editing, formatting and proof reading. Using this free service, authors can make their results available to the community, in citable form, before we publish the edited article. We will replace this *Accepted Manuscript* with the edited and formatted *Advance Article* as soon as it is available.

You can find more information about *Accepted Manuscripts* in the [Information for Authors](#).

Please note that technical editing may introduce minor changes to the text and/or graphics, which may alter content. The journal's standard [Terms & Conditions](#) and the [Ethical guidelines](#) still apply. In no event shall the Royal Society of Chemistry be held responsible for any errors or omissions in this *Accepted Manuscript* or any consequences arising from the use of any information it contains.

TOC Entry



A network of process-based mass-balance models for phosphorus dynamics in catchments and lakes provides a new approach to simulate the effect of land-use and climate change on water quality.

Environmental impact statement

Computer-based environmental modelling offers an essential aid to understand current catchment dynamics and to investigate the potential effectiveness of remedial actions aimed at improving water quality. Here, we present a novel network of processes-based, mass-balance models linking climate, hydrology, catchment-scale P dynamics and lake processes. This study exemplifies how an objectively calibrated model network allows disentangling the effects of climate change from those of land-use change on lake water quality and phytoplankton growth. The model network can thus support decision-making to reach good water quality and ecological status.

1 *Modelling Phosphorus Loading and Algal Blooms in a Nordic*
2 *Agricultural Catchment-Lake System Under Changing Land-use*
3 *and Climate*

4 **Authors**

5 Raoul-Marie Couture^{1,2}, Koji Tominaga^{1,3}, Jostein Starrfelt¹, S. Jannicke Moe¹, Øyvind
6 Kaste¹, Richard F. Wright¹

7 1- Norwegian Institute for Water Research, Gaustadalléen 21, 0349 Oslo, Norway.

8 (✉)E-mail: rmc@niva.no

9 2- University of Waterloo, 200 University Avenue West, N2L 3G1 Waterloo, Canada.

10 3- Centre for Ecological and Evolutionary Synthesis (CEES), Dept. of Biosciences,
11 University of Oslo, P.O.Box 1066, 0316, Oslo, Norway

12 **Abstract**

13 A model network comprising climate models, a hydrological model, a catchment-scale
14 model for phosphorus biogeochemistry, and a lake thermodynamics and plankton dynamics
15 model was used to simulate phosphorus loadings, total phosphorus and chlorophyll
16 concentrations in Lake Vansjø, southern Norway. The model network was automatically
17 calibrated against time series of hydrological, chemical and biological observations in the
18 inflowing river and in the lake itself using a Markov Chain Monte-Carlo (MCMC)
19 algorithm. Climate projections from three global climate models (GCM: HadRM3,
20 ECHAM5r3 and BCM) were used. The GCM model HadRM3 predicted the highest increase
21 in temperature and precipitation, and yielded the highest increase in total phosphorus and
22 chlorophyll concentrations in the lake basin over the scenario period of 2031-2060. Despite
23 the significant impact of climate change on these aspects of water quality, it is minimal
24 when compared to the much larger effect of changes in land-use. The results suggest that
25 implementing realistic abatement measures will remain a viable approach to improving
26 water quality in the context of climate change.

27 **Introduction**

28 The use of the nutrient phosphorus (P), an essential fertilizer element enhancing plant
29 growth, has underpinned global agriculture and food production since the beginning of the
30 20th century. Global P-based food production, which has doubled over the past 45 years¹,
31 has been hypothesized to be responsible for the estimated three-fold increase in the river
32 borne flux of P to the oceans since pre-industrial times (*e.g.*, Haygarth²). When P is
33 delivered to water bodies, negative influences on water quality are likely, and the
34 eutrophication of freshwater and coastal marine ecosystems resulting from increased
35 anthropogenic P loadings is a global problem³. In lake basins specifically, excess nutrients
36 from both point and nonpoint sources throughout the catchment can give rise to harmful
37 algal blooms, degrade water quality, and create extensive oxygen depletion.

38 The discharge of P to surface water is subject to comprehensive regulations worldwide,
39 such as the Clean Water Act (CWA) in the USA, Water Pollution Prevention and Control
40 (WPPC) Law in China and the Water Framework Directive (WFD) in the European Union.
41 In Europe, the WFD 2000/60/EC has been designed to achieve good biological and chemical
42 status for water bodies by 2015⁴, promoting an approach to water and land management
43 through river basin planning explicitly aimed at reducing the impacts of eutrophication
44 caused by excess nutrient inputs.

45 Climatic conditions –in addition to land use, agricultural practices, urban and sewage
46 nutrient inputs– are key drivers of eutrophication in lakes⁵⁻⁸. For instance, in a given
47 catchment, air temperature, precipitation, and the morphometry of a lake will determine the
48 extent to which wind-mixing will influence the vertical transfer of P and influence the effect
49 of light on P uptake by phytoplankton. In the context of climate change, it is becoming
50 increasingly difficult to disentangle the complex climatic effects influencing water quality
51 from the effects of specific measures implemented to improve it⁹. A better understanding of
52 the response of specific catchments to both climate and land-use change is needed for a
53 scientifically-guided management design to mitigate the impact of these changes on water
54 quality.

55 Computer-based environmental modelling offers an aid to understanding current
56 catchment dynamics and investigating the potential effectiveness of remedial actions in the
57 context of climate change. Building on previous catchment modelling efforts aiming at
58 predicting P delivery to lakes in agricultural catchments,¹⁰⁻¹³ we constructed a novel network
59 of chained model to integrate climate, hydrologic, catchment, and in-lake processes. At the
60 top of the model chain is a global climate model (GCM) whose output for daily temperature,
61 precipitation and other variables were downscaled to the region. These are used as inputs to
62 a hydrologic rainfall-runoff model (PERSiST¹⁴) to produce daily discharge values for rivers,
63 which, in turn, are used as inputs for INCA-P¹⁵ to simulate daily fluxes suspended sediments
64 and P to the lake. At the end of the model chain is the lake model MyLake¹⁶. Here, we take
65 advantage of these models' matching state variables, spatial scales and temporal
66 resolutions¹⁷, and couple them into a network consisting of river stretches and lake basins,
67 and to perform automated calibration and uncertainty analysis across the network. The

68 seamless connection between model components allows for the propagation of changes in
69 boundary conditions –such as climatic or land-use changes– within the model network (*e.g.*,
70 Voinov¹⁸). The model network is applied to the Vansjø-Hobøl catchment (Norway), whose
71 water quality, nutrient loading¹⁹, as well as past and recent land-uses have been thoroughly
72 documented due to the basin's pivotal importance for water supply and its sensitivity to
73 eutrophication in lake Vansjø²⁰.

74 The main anthropogenic pressure on the Vansjø-Hobøl catchment is a surplus of P,
75 which has resulted in eutrophication and severe blooms of cyanobacteria, including the
76 potentially toxic *Microcystis*^{7, 19-23}. Although it is generally recognized that the abundance of
77 the essential nutrient nitrogen (N) and silicon (Si) are also key factors controlling algal
78 growth and thus water quality^{24,25}, our work has focussed on P based on evidence that
79 phytoplankton growth in this system is P-limited¹⁹. As agricultural practices continue to
80 expand in the basin, and with the observed increase in temperature and precipitation in
81 northern Europe²⁶, the occurrence of algal blooms is expected to increase. We thus aimed to
82 model the response of biological (*i.e.*, chlorophyll) and chemical (*i.e.*, phosphorus)
83 indicators of water quality, as defined by the WFD, to climate and land-use changes in the
84 Vansjø-Hobøl catchment and to assess the influence of climate change on the feasibility of
85 reaching existing water quality targets.

86

87 **Material and methods**

88 **2.1 Site description**

89 The Vansjø-Hobøl catchment (area = 690 km²), also referred to as the Morsa
90 catchment, is located in south-eastern Norway (59°24'N 10°42'E). The Hobøl River, with a
91 mean discharge of 4.5 m³ s⁻¹, drains a sub-catchment of 301 km² into Lake Vansjø, the
92 catchment's main lake. Lake Vansjø has a surface area of 36 km² and consists of several
93 sub-basins, the two largest being Storefjorden (eastern basin, L1 in Fig. 1) and
94 Vanemfjorden (western basin, L2 in Fig. 1), whose characteristics are described in Table 1.
95 The water-column of both basins remains oxygenated throughout the year. In addition, there
96 are six smaller lakes which together represent less than 15% of the lake surface area. The
97 Storefjorden basin drains to the Vanemfjorden basin through a shallow channel. The outlet
98 of Vanemfjorden discharges into the Oslo Fjord (Fig. 1).

99 **2.2 The model network**

100 The model network consists of four separate models: a climate model, a hydrological
101 model, a catchment model for P, and a lake model. The model network is first calibrated to
102 present-day observed data, then run with four storylines to simulate conditions in the future.
103 The model network is shown in Fig. 1 and described in detail below.

104 **Climate models.** For a given greenhouse gas emission scenario (see section 2.4),
105 projections of future climate change differ depending on the GCM used²⁷. Consequently, we
106 tested the following three GCMs independently as inputs: (1) HadCM3²⁸, (2) ECHAM5²⁹,
107 and (3) Bergen Climate Model (BCM)^{30,31}. The outputs from the GCMs were the basis for
108 RCMs, yielding dynamically-downscaled daily weather projections. Details on the GCM-
109 RCM pairs are given in Table 2. This approach has been shown to be an effective way to
110 couple climate with hydrology³².

111 **Catchment models.** The outputs of the RCMs, together with basin characteristics, were
112 used as inputs for the hydrological PERSiST model to produce daily estimates of runoff,
113 hydrologically effective rainfall and soil moisture deficit. Previously, external time series of
114 runoff, hydrologically effective rainfall and soil moisture deficits have been obtained from
115 rainfall-runoff models such as HBV³³. Here, we use instead the new model PERSiST v.
116 1.0.17¹⁴, a daily-time step, semi-distributed rainfall-runoff model designed specifically for
117 use with INCA models. Although PERSiST shares many conceptual characteristics with the
118 HBV model, such as the temperature index representation of snow dynamics and
119 evapotranspiration, it differs in its description of water storage¹⁴. PERSiST uses the same
120 conceptual representation of water storage as the INCA models. Coupling PERSiST with
121 INCA allows a consistent conceptual model of the runoff generation process for both
122 hydrological estimations and water chemistry simulations.

123 **Water chemistry models.** Daily hydrological outputs from PERSiST, and weather forcing
124 from the RCMs, were used as inputs for INCA-P. The catchment P-dynamic model INCA-
125 P¹⁵, one of the iterations of the INCA-suite of models, is a process-based, mass balance

126 model that simulates temporal variation in P export from different land-use types within a
127 river system. It has been used extensively in Europe and North America to simulate P
128 dynamics in soils and surface waters and to assess the potential effects of climate and land
129 management on surface water quality^{7, 11-13, 15, 34, 35}. We use a recent fully-branched version
130 of INCA-P¹¹ (Branched-INCA-P v. 0.1.31), in which reaches are defined as stretches of
131 river between two arbitrarily defined points, such as a gauging station, a topographic feature
132 or a lake basin. INCA-P is so-called semi-distributed, that is, soil properties are spatially
133 averaged within user-defined sub-catchments branches. It produces daily estimates of
134 discharge (Q , $\text{m}^3 \text{d}^{-1}$), concentration of suspended solids (SS, mg L^{-1}), soluble reactive P
135 (SRP; $\mu\text{g L}^{-1}$) and total phosphorus (TP; $\mu\text{g L}^{-1}$). The application here (Fig. 1) simulates the
136 7 catchment reaches: five reaches of the Hobøl River catchment, each with defined land-use
137 and hydrology (R1-R5); the local Storefjorden sub-catchment (R6); and the Vanemfjorden
138 sub-catchment (R7). The multi-branch reach structure was established using GIS and land-
139 use maps for the area (Section 2.3) and the location of monitoring stations and discharge
140 point into lake basins¹¹.

141 **MyLake model.** The lake model used, MyLake v. 1.2.1, is a one-dimensional process-based
142 model designed for the simulation of seasonal ice-formation and snow-cover in lakes, as
143 well as for simulating the daily distribution of heat, light, P species, and phytoplankton
144 abundance in the water column¹⁶. MyLake has been successfully applied to several lakes in
145 Norway, Finland and Canada^{16, 36, 37} to simulate lake stratification and ice formation^{16, 36, 37}.
146 It uses daily meteorological input data such as global radiation (MJ m^{-2}), cloud cover, air
147 temperature ($^{\circ}\text{C}$), relative humidity (%), air pressure (kPa), wind speed (m s^{-1}) and
148 precipitation (mm), as well as inflow volumes and P fluxes to produce daily temperature (T,
149 $^{\circ}\text{C}$) profiles in the water column, concentration profiles and outflow concentrations of SS,
150 dissolved inorganic P ($\text{PO}_4\text{-P}$, $\mu\text{g L}^{-1}$), particulate inorganic P (PIP, $\mu\text{g L}^{-1}$), dissolved
151 organic P (DOP, $\mu\text{g L}^{-1}$), chlorophyll- α (Chl, $\mu\text{g L}^{-1}$) and TP. The biogeochemical processes
152 linking these state variables in the water-column are the mineralisation of DOP and of Chl to
153 PO_4 , and the removal of PO_4 through phytoplankton growth (yielding Chl) or through
154 sorption onto SS (yielding PIP). In the sediments, mineralisation of organic-P and
155 equilibrium partitioning of PIP to the pore water governs the fluxes of PO_4 to the to the
156 water-column, while resuspension allows Chl and PIP to return to the bottom water. Details
157 on the equations governing these processes are given in Saloranta and Andersen¹⁶. In the
158 MyLake model, phytoplankton has a constant C:P ratio of 106:1 and a organic-P:Chl ratio of
159 1:1, such that particulate organic-P is a proxy for Chl. Similar stoichiometries and constant
160 P:Chl ratios can be found in other models for lake plankton dynamics, such as PROTECH²⁵.
161 Finally, total particulate P ($\text{PP} = \text{TP} - \text{PO}_4$; $\mu\text{g L}^{-1}$) was calculated offline and compared to
162 field observations (see section 2.3) to calculate performance metrics.

163 MyLake was set-up for 2 lake basins (Fig. 1), Storefjorden (L1) and Vanemfjorden
164 (L2). The outputs of the R1 to R6 simulations from INCA-P are combined and used as
165 inputs for L1. L1 and R7 are then combined and used as inputs for L2. The MyLake setups
166 L1 and L2 are at the end of the model chain, because the lake Vanemfjorden (L2) discharges
167 in the Oslo fjord.

168 **2.3 Model input**

169 Observed climate, precipitation, temperature and wind data at Lake Vansjø were
170 obtained from daily weather data at the Norwegian Meteorological Institute stations (1715
171 Rygge; 1750 Fløter; 378 Igsi) located between the Vanemfjorden and Storefjorden basins
172 (59°38'N, 10°79'E). These data were used as the common atmospheric forcing throughout
173 the study; either as is for present-day climate or scaled using the RCM predictions for
174 climate change scenarios (see section 2.4). Catchment hydrology was constrained using
175 daily flow measured at the gauging station at Høgfoss (Station #3.22.0.1000.1; Norwegian
176 Water Resources and Energy Directorate, NVE).

177 The land cover structure for the Vansjø-Hobøl catchment was constructed from GIS
178 digital terrain elevation maps provided by the Norwegian Forest and Landscape Research
179 Institute and complemented by a recent report on the fertilization regimes of agricultural
180 fields²⁰. Historical nutrient outputs from waste-water treatment plants (WWTPs) were
181 obtained from the online database KOSTRA, maintained by Statistics Norway
182 (<http://www.ssb.no/offentlig-sektor/kostra>). TP and SS data were analysed downstream of
183 Høgfoss, at Kure³⁸. P loadings from scattered dwellings are provided by the online GIS
184 information system GISavløp maintained by the Norwegian Institute for Agricultural and
185 Environmental Research (Bioforsk; <http://www.bioforsk.no/webgis>). Land cover of the
186 Vansjø-Hobøl catchment is dominated by forestry (78%), agriculture (15%) and water
187 bodies (7%). The agricultural land-use is dominated by cereal production (89%), with a
188 smaller production of grass (9.8%), vegetables (0.6%) and potatoes (< 0.1%). Together,
189 agricultural practices contribute an estimated 48% of the total P input to the river basin,
190 followed by natural runoff (39%) and WWTPs (5%) and scattered dwellings (8%). It is
191 estimated that these external sources of P contribute to the majority of the P loads to Lake
192 Vansjø²⁰.

193 For the Vanemfjorden and Storefjorden basins, water chemistry and temperature data
194 were provided by the Vansjø-Hobøl monitoring program, conducted by Bioforsk and by the
195 Norwegian Institute for Water Research (NIVA). Water-column sampling was conducted
196 weekly from 1990 to 2004, and bi-weekly from 2004 on, at the deepest-site of both basins
197 whose coordinates are given in Table 1, using a depth-integrating pipe water-column
198 sampler positioned at 2-4 m depth. Values of TP, PP, Chl and PO₄ water-column
199 concentrations for both basins are accessible through NIVA's online database
200 (<http://www.aquamonitor.no>).

201 **2.4 Scenarios and storylines**

202 Scenarios are valuable to evaluate alternative directions for development and policy
203 implementation. Here, we have defined scenarios representing possible futures in global and
204 regional climate and in catchment management. We combine these climate predictions and
205 management scenarios into storylines, which help convey the output of the simulations into
206 quantitative expectations for future P loadings in the Vansjø catchment (Fig. 2). The
207 assumptions made in defining these scenarios, and the choice made to combine them into
208 storylines, are detailed below.

209 **Climate.** Three GCMs were used to obtain predictions according to the A1B greenhouse gas
210 emission scenario (2030-2052) of the Intergovernmental Panel on Climate Change (IPCC)²⁷.
211 The A1 scenario family describes a future world of rapid economic and population growth,
212 and the introduction of new and more efficient technologies. It is subdivided into groups that
213 describe alternative directions of technological change in the energy system. The A1B sub-
214 scenario, which describes a balance between a growing reliance on fossil energies and an
215 emergence of new technology, assuming that similar improvement rates apply to all energy
216 supply and end-use technologies. This scenario projects that anthropogenic emission of
217 greenhouse gases (CO₂, CH₄ and N₂O) peaks and begins to decline past the year 2050. GCM
218 runs, prepared from the results of the ENSEMBLES EU FP6 project^{39, 40} provided boundary
219 conditions for the RCMs. The outputs of these model pairs, all based on the A1B scenario of
220 climate change, are hereafter referred to as future climates C1-C3 (Table 2 and Fig. 3),
221 whereas the climate condition during the reference period (1990-2012) is referred to as
222 climate C0 .

223 Because the RCMs were based on spatial domains much larger than the catchment, they may
224 contain seasonal biases. Consequently, RCM outputs for the Vansjø-Hobøl catchment were
225 bias corrected on a monthly basis. Daily resolution scenario data for surface air temperature
226 and precipitation were derived from a sub-set of these regional climate model simulations⁴¹
227 and implemented by scaling the observed weather (1990-2012). Observed temperatures were
228 changed to reflect both the increase in median and variance predicted by the climate models.
229 Precipitation was scaled using a ratio of change approach, multiplying observation by the
230 ratio of observed (1990-2012) over predicted (2030-2052) precipitation. Averaged, monthly
231 local changes in temperature and precipitation predicted by the three RCMs under the A1B
232 scenario for the 2030-2052 period are shown in Fig. 3. Overall, HadRm3 predicts average
233 yearly changes in both temperature and precipitation that are greater than those predicted by
234 ECHAM5 or BCM (Table 2).

235 **Management.** Three management scenarios were developed together with stakeholders
236 involved in the catchment's land-use and water management. As a result, the following
237 scenarios represent realistic actions that the stakeholders have the capacity to implement.
238 The reference scenario (M0) represents historical riverine nutrient concentrations and
239 current loadings from land-use, fertilization and WWTPs. The sustainable management
240 scenario (M1), referred to as "water-quality focus", represents the implementation of
241 measures to further mitigate the risk of eutrophication in the catchment. These measures
242 impose: (1) a 10% reduction in agricultural land, which is then converted to forest, (2) a
243 25% decrease in vegetable production, which is then converted to grass production, (3) a
244 25% decrease in P-based fertilizer application, and 4) a 90% improvement in the P-
245 removing performance of WWTPs. Finally, a less sustainable management scenario (M2),
246 referred to as "economic focus", reflects a projected increase in anthropogenic pressure
247 throughout the catchment due to population growth and an intensification of food
248 production. Further growth of agricultural and urban activities in the catchment in scenario
249 M2 are imposed as follows: (1) a 10% reduction of forest cover, which is then converted to
250 agricultural lands, (2) a shift of 25% of the grass production to vegetable production, (3) an

251 increase of fertilizer application by 25%, and (4) a 25% increase in the P load of effluents
252 from scattered dwellings and WWTPs throughout the catchment.

253 **Storylines.** The management scenarios M1 and M2 were either considered with the
254 reference climate (C0) or with future climate change, thus defining 4 storylines which
255 represent the possible combined effects of climate change and management practices in the
256 Vansjø-Hobøl catchment (Fig. 2). Storylines 1 and 2 encompass the water-quality focus
257 scenario with and without climate change, respectively, while Storylines 3 and 4 encompass
258 the economic focus scenario with and without climate change, respectively. The Reference
259 storyline represents the present climate conditions combined with the historical management
260 of the catchment.

261 **2.4 Calibration and uncertainty analysis**

262 PERSiST was manually calibrated against measured stream flow in the Hobøl river
263 at the end of reach R4 for the observation period of 1 January 1996 to 3 December 2000.
264 The INCA-P and MyLake models were calibrated using a Markov Chain Monte Carlo
265 (MCMC) approach. Given the large number of parameters involved in the simulation of 7
266 river reaches and 2 lake basins using INCA-P and MyLake, probably many alternative sets
267 of parameters could achieve the same degree of fit with observed data. Manual calibration
268 identifies only one possible set, and perhaps not the best fit, while locally scoped and
269 uniquely defined auto-calibration software, such as PEST, would fail to adequately address
270 multimodality and equifinality⁴². To capture the envelope of acceptable parameter sets
271 systematically throughout the parameter combination space, a probabilistic calibration was
272 performed using a Bayesian inference scheme, where each parameter was given a prior
273 distribution and a posterior distribution using a recent MCMC approach, within the
274 framework of a self-adaptive differential evolution learning scheme (DREAM)⁴²
275 implemented in MATLAB (Starrfelt et al., this issue).⁶⁸ The calibration was performed by
276 choosing site-specific parameters, which are not known with certainty beforehand, and
277 allowing those values to vary within the parameter space.

278 INCA-P (28 parameters varied) was calibrated by calling the MCMC-DREAM
279 algorithm described in Starrfelt et al. (this issue)⁶⁸ against \log_{10} -transformed time series
280 acquired at R4 (Fig. 1) for the observation period of 1 December 1992 to 31 January 1995.
281 After calibration, parameter sets from the last iterations were sampled and the model was
282 run for the scenario period and over the whole catchment. Median simulated values from
283 ~600 runs per scenarios were then passed to MyLake. MyLake (10 parameters varied) was
284 calibrated against a time series of measurements in the surface waters of the Vanemfjorden
285 and the Storefjorden basins for the observation period of 1 April 2005 to 1 September 2012.
286 Technical details on the sensitivity and uncertainty analysis of such a model network are
287 given elsewhere⁴³.

288 The goodness of fit between observations in the catchment and the model predictions
289 from PERSiST and INCA-P, as well as between observations in the lake water columns and
290 the model predictions from MyLake, were evaluated using the coefficient of determination

291 (R^2), the root-mean-square error (RMSE) and the Nash-Sutcliffe coefficient (NS) statistic.
 292 The latter was calculated both on normal and on log-transformed values. These metrics were
 293 chosen because they represent the following three major categories of model performance
 294 metrics⁴⁴: (1) standard regression statistics to determine the strength of the linear
 295 relationship between simulated and measured data (*i.e.*, R^2), (2) error indices to quantify the
 296 deviation in the units of the data of interest (*i.e.*, RMSE) and (3) dimensionless techniques to
 297 provide a relative model evaluation assessment (*i.e.*, NS). R^2 values range from 0 to 1, with
 298 higher values indicating less error variance, and typically values greater than 0.5 are
 299 considered acceptable. RMSE values retain the same units as the constituent being
 300 evaluated, and can be directly compared with the data (as in Figs. 4 and 5). A RMSE value
 301 of 0 indicates a perfect fit. NS ranges between $-\infty$ and 1, with a value of 1 being optimal and
 302 values between 0.5 and 1 being generally viewed as good. Negative NS values indicate that
 303 the mean observed value is a better predictor than the simulated value, pointing to poor
 304 model performance. We refer the reader to Moriasi⁴⁴ for extensive discussion on the
 305 procedures used to qualify the calculated values of these statistics.

306 In addition to the performance metrics described above, “target diagrams”^{45, 46} were
 307 used to compare the model’s performance with respect to Q, TP, Chl and PO_4 . Target
 308 diagrams conveniently represent aggregated performance metrics by plotting the normalized
 309 bias (B^* , where * denotes normalization) against the normalized unbiased root mean square
 310 difference ($RMSD'^*$)^{43, 44}. B^* is defined as:

$$311 \quad B^* = \frac{\frac{1}{N} \sum_{n=1}^N (M_n - D_n)}{\sigma_D} \quad \text{Eq. 1}$$

312 where N is the total number of observations and model output pairs, D_n is the observation at
 313 each site, M_n is the corresponding model output, and σ_D is the annual standard deviation of
 314 the observed data. $RMSD'^*$ is calculated as follow:

$$315 \quad RMSD'^* = \frac{sgn(\sigma_M - \sigma_D)}{\sigma_D} \left[\overline{(M'_n - D'_n)^2} \right]^{0.5} \quad \text{Eq. 2}$$

316 where *sgn* represents the sign of the standard deviation difference and σ_M the annual
 317 standard deviation of the modelled data. If the model standard deviation is greater than the
 318 observation standard deviation, $RMSD'^*$ is positive.

319 **3. Results and Discussion**

320 **3.1. Model performance**

321 The hydrology of the catchment was well simulated with PERSiST and yielded
 322 satisfactory fits to the observed discharge (Fig. 4), as reflected by the high NS coefficient ($>$
 323 0.85; Table 3). The hydrological model HBV³³, previously used in conjunction with INCA-
 324 P, yielded similarly satisfactory simulations of flows¹⁷. Although the use of log-transformed
 325 values yielded satisfactory fits with respect to NS_{\log} for both Q and TP, the INCA-P
 326 calibration against TP measurements is characterized by relatively poor performance metrics

327 (Table 3, Fig. 4). Here, we aimed for a compromise between performance in some
328 components of the individual models and a realistic propagation of the changes in boundary
329 conditions through the integrated system across the model components, as discussed in
330 Voinov¹⁸.

331 The water quality simulated by MyLake during the calibration period for the surface
332 waters of Storefjorden (L1) and Vanemfjorden (L2) are shown in Fig. 5, and the
333 corresponding model performance statistics are summarized in Table 3. The observed P
334 dynamics in both basins display strong seasonal features, with TP, Chl, and PP all reaching
335 maximum values during the summer, when the lake productivities are at their highest.
336 Conversely, PO₄ is at a minimum during the summer, consistent with its uptake by
337 phytoplankton. Observed TP values show a high degree of variability from week-to-week,
338 likely due to the integrating nature of the TP parameter. Visual inspection of Fig. 5 shows
339 that MyLake simulations for both basins well captured the seasonal minima in PO₄ and
340 maxima in both PP and Chl. The seasonal trends in Chl, a measure of the abundance of
341 phytoplankton, are also well captured by the model, with the exception of an algal bloom in
342 the summer of 2006, whose magnitude was not fully captured (Fig. 5). The algal bloom in
343 the summer of 2008 is reproduced by the model, although also underestimated, despite the
344 high magnitude rain events that occurred throughout the catchment during that year. In
345 particular, a single bank erosion event in the winter of 2008 resulted in high SS in the
346 river²². The NS metric is high for simulated Q with PERSiST, but low for simulations of TP
347 with both INCA-P and MyLake (Table 3). This metric is unforgiving, in that it is strongly
348 affected by simulations that do not match observed peak concentrations.

349 The target diagrams (Fig. 6) allow for the comparison of model performance among
350 parameters and stations in a normalized manner, independent of the magnitudes of the
351 simulated values. The RMSD'* calculation involves the multiplication of a term in Eq. 2 by
352 the sign of difference between the standard deviation (σ) of simulations and observations. As
353 a result, the RMSD'* provides information about whether the σ of simulated values is larger
354 or smaller than σ of the observations. An increase in RMSD'* reflects an increase in the
355 discrepancy between simulations and observations⁴⁶, pointing to incommensurability
356 between what is modelled and the available observations, while lower values indicate less
357 residual variance between them. B* represents systematic over- or under-estimation of the
358 simulated vs observed values. Fig. 6 reveals that the simulations are generally unbiased, and
359 that the residual variances increase as we move from INCA-P to MyLake, that is, further
360 along the model network. When compared to the observations, INCA-P simulations are less
361 biased and, on an absolute scale, have a smaller RMSD'* than the simulations generated by
362 MyLake. This information was not revealed solely by calculating the metrics reported in
363 Table 2.

364 Despite the low NS metrics reported for INCA-P, three lines of evidence suggest that
365 the model delivers representative TP loads to the lake model: (1) a linear regression of
366 cumulative TP loads estimated from observed Q and TP vs those predicted by INCA-P
367 yields a R² of 0.90 ($n=124$, $p<0.05$), (2) the B* and RMSD'* values obtained when

368 comparing estimated and predicted TP loads are low (Fig. 6), and (3) the performance of the
369 lake models is acceptable. Previous –although simpler– INCA-P setups calibrated on data
370 from other Norwegian catchments^{35, 47} were also deemed satisfactory when evaluated
371 against fortnightly or monthly TP loads rather than daily TP values. Thus, during the
372 scenario period, the response of INCA-P to the climate and land-use changes is expected to
373 be reasonable both in magnitude and in direction.

374 MCMC-DREAM analysis provides information on the sensitivity of the simulations
375 to INCA-P and MyLake parameters. For INCA-P, of the 28 parameters tested, TP
376 concentrations were most sensitive to parameters controlling hydrology and erosion across
377 the different land-uses, in particular the soil reactive zone time constant (d^{-1}) –which in
378 INCA refers to the amount of water present in the soil and its residence time–, the soil
379 erodibility ($kg\ m^{-2}\ d^{-1}$), the direct runoff time constant, and the base flow index.
380 Downstream, P speciation predicted by MyLake was most sensitive to 5 out of the 10
381 parameters tested: the re-suspension rate of sediments ($m\ d^{-1}$), the sinking rate of suspended
382 inorganic particles ($m\ d^{-1}$), the algae growth rate (d^{-1}), the heat vertical diffusion coefficient,
383 and the wind sheltering coefficient. P speciation was moderately sensitive to the sinking rate
384 ($m\ d^{-1}$), the sorption coefficient of P onto inorganic particles ($mg\ P\ m^{-3}$), and to the algae
385 mortality rate (d^{-1}), while insensitive to PAR saturation ($mol\ quanta\ m^{-2}\ s^{-1}$) and snow
386 albedo. The co-variance structure in the parameter space gathered by applying MCMC-
387 DREAM analysis is described elsewhere for INCA-P (Starrfelt et al. [this issue](#))⁶⁸ and
388 MyLake⁴³.

389 **3.2. Impact of climate and land-use change on water quality**

390 Several P-mitigation measures have been implemented in the Vansjø-Hobøl
391 catchment over recent decades. These measures consist of reduced tillage to control erosion,
392 reduced fertilizer application rate, implementation of vegetated buffer strips along most of
393 the streams in cultivated areas, construction of artificial wetlands, and incremental
394 improvement of WWTP performance^{20, 21}. As a result, TP loads and Chl concentrations
395 steadily decreased throughout the reference period (Fig. 7). Imposing the storylines
396 described in section 2.4 on these historical reference conditions reveals: i) what the water
397 quality status in the Vansjø-Hobøl catchment would have been should additional
398 management decisions have been made, and ii) the effect of different climate change
399 scenarios on water quality.

400 PERSiST and INCA-P predict that the hydrological response to climate change
401 causes a significant increase in runoff and in the fluxes of TP to the lake basins. This result
402 is consistent with observations in Danish lakes⁵ where higher TP loads were ascribed to
403 climate-induced increases in rainfall. MyLake output indicated no significant differences
404 between the thermocline depths predicted under climate change and those predicted under
405 present-day climate conditions (t-test, $n = 523$, $p > 0.05$). This suggests that changes in air
406 temperature and precipitation in Storyline 2 and 4 do not induce significant variations in the
407 water-column structures at the scale modelled by MyLake (i.e., vertical resolution of 1m).
408 On the other hand, ice cover duration was predicted by MyLake to decrease significantly (p

409 < 0.05) under climate change; indeed, MyLake projected shorter duration of ice cover for
410 lakes in the entire Nordic region³⁷. For a given management scenario, TP and Chl values
411 predicted under climate change were significantly higher (t-test, $n = 523$, $p < 0.05$) than
412 those predicted using present-day climate conditions (96% of the times for Chl and 76% of
413 the times for TP). Amongst the three climate models tested, HadRm3 (C1) projected the
414 largest climate change³⁹, and yielded the highest TP and Chl values. Most likely this was
415 due to the higher amount of precipitation projected by HadRm3, which resulted in higher P
416 loads and runoff from the catchment in INCA-P.

417 The increase in Chl production predicted by MyLake was higher in the summer
418 months (Fig. 8). The model's handling of phytoplankton growth, which is temperature-
419 driven when neither light nor PO_4 is limiting¹⁶, explains this result. Recent studies have
420 further highlighted that temperature-mediated P release from lake sediment can increase
421 under a warmer climate^{5, 6, 48}, thus furthering algal growth. However, the influence of higher
422 temperatures on internal P loadings in Lake Vansjø cannot be ascertained here, because the
423 relevant sediment-water processes are only partly implemented in the MyLake model (See
424 section 3.4). In addition, the climate scenario used here, A1B, predicted that greenhouse gas
425 emissions will be curbed by the mid-21st century. Other scenarios, such as those in the A2
426 and B2 families of scenarios, assume larger increases of greenhouse gases emissions as well
427 as higher increases in temperature and precipitation in Nordic catchments. The outcome of
428 our simulations indicates that these climatic conditions would further increase the risk of
429 eutrophication in Nordic lakes, as previously suggested^{6, 12, 49, 50}. Thus, projected increases of
430 Chl concentrations are likely conservative.

431 In general, any given management scenario resulted in higher TP and Chl
432 concentrations when climate change was included. This is seen for the Storefjorden basin in
433 the years following 2040, for which the detrimental effect of climate change overrides the
434 beneficial effects of the water-quality focus storylines. Both TP and Chl reach values above
435 those of the reference storylines, for which no additional P-load reduction was imposed.
436 Nonetheless, and although the effects of climate change are significant, variations in water
437 quality brought about by different management scenarios are always greater than those
438 brought about by climate change (Fig 7). Land-use and management regimes had a profound
439 impact on water quality, more so than the projected climate change under the A1B scenario.
440 Relative to the reference storyline, imposing a water-quality focus (Storyline 1) improved
441 the water quality overall by decreasing TP and Chl by 24% and 33%, respectively, in
442 Storefjorden, and by 18% and 23%, respectively, in Vanemfjorden. Conversely, an
443 economic focus (Storyline 3) adversely affected water quality by increasing TP and Chl by
444 58% and 59%, respectively, in Storefjorden, and by 44% and 42%, respectively, in
445 Vanemfjorden. It thus follows that Storyline 1 represents the best case, while Storyline 4
446 represents the worst case (Fig 2).

447 **3.3 Implications of climate and land-use change for water management**

448 The seasonal distributions of the daily predicted TP and Chl concentrations (Fig. 8)
449 show that the water quality is much worse during the summer months under all storylines.

450 Using the lake-specific water quality thresholds of the WFD⁵¹, we calculated the proportion
451 of simulated days for which the regulatory thresholds for good/moderate and moderate/bad
452 water quality were exceeded. These thresholds are specific to each lake type, so that the TP
453 and Chl concentrations below which the water quality meets the guideline are different for
454 Storefjorden and Vanemfjorden (Table 4).

455 The water-quality focus scenario without climate change (Storyline 1) increases the
456 number of days for which the concentrations of TP and Chl are deemed “good”, and has a
457 greater influence on Chl than for TP (Table 4). Nevertheless, the “good/moderate” water
458 quality threshold will still be exceeded 98-99% of the time for TP and 88-90% of the time
459 for Chl. Under an economic focus scenario with climate change (Storyline 4), the water
460 quality degrades such that the concentrations of both TP and Chl exceed the moderate/bad
461 threshold values 99% of the time in the summer. Together, these results suggest that it will
462 be difficult to reach the environmental targets set for TP and Chl in Lake Vansjø under the
463 European WFD, even under the best-case scenario represented by Storyline 1. More
464 stringent water-quality focused measures are, therefore, likely needed. Arguably, a full
465 assessment of the compliance of water quality indicators to the WFD directive requires
466 greater details regarding algal species assemblages, in particular observations and
467 predictions regarding the abundance of potentially harmful algae such as cyanobacteria,
468 which in addition to higher TP levels are expected to be stimulated by increased
469 temperature⁵².

470 *3.4 Sources of uncertainty*

471 Assessing the level of uncertainty in the outcome of an environmental model
472 provides a forthright basis for decision-making and regulatory formulation. The sources of
473 uncertainty in water quality modelling at the river-basin scale range from uncertainty linked
474 to the choice of processes represented, the uncertainty in the model parameters and the data
475 themselves. Here, uncertainty was assessed by performing auto-calibration (see section 2.4)
476 and accepting as usable those parameter sets yielding simulations of equal likelihood. This
477 uncertainty is represented by the interquartile space shown on Fig. 5. Overall, the
478 uncertainty in Chl predictions are greatest around the time where its level peaks during
479 spring and summer months (Fig. 5). Conversely, the model generally agreed with the
480 observation on the timing of the clear water period occurring between the spring and
481 summer blooms, as the uncertainty band visibly narrows around the simulated median (Fig.
482 5). For the scenario simulations, the uncertainty was largest for scenarios where climate
483 change and increased external nutrient loads were combined, relative to the scenarios with
484 climate change alone. MyLake’s predictions of phytoplankton abundance thus bear greater
485 uncertainty at higher biomass levels.

486 In addition to estimating uncertainty statistically, we identified shortcomings in the
487 models that likely introduce further uncertainty in the predictions. As mentioned above,
488 INCA-P predictions are sensitive to soil erosion parameters. INCA-P is somewhat limited in
489 its handling of erosion processes and of particle transport, resulting in an increased

490 uncertainty surrounding its predictions. Erosion events generating pulses of particles, such
491 as landslides, have been observed in the Vansjø-Hobøl catchment, for instance in 2008²⁰,
492 when river bank erosion occurred following a flood and temporarily increased the particle
493 load into the Storefjorden basin. The effect of bank collapse on runoff and particle transport
494 is not spatially represented in INCA and particle retention measures, such as sedimentation
495 ponds and buffer strips, cannot be explicitly represented in the model. Although such
496 structures are better modelled using fully-distributed codes⁵³, their effect on P migration in
497 the catchment and on erosion control remain problematic to model because landscapes are
498 not at steady-state, and are subject to tipping points under increasing climatic pressures⁵⁴
499 and extreme hydrologic events. Finally, INCA-P is a rather heavily parameterized model,
500 and the lack of data on some of the processes represented in the model introduces
501 uncertainty. Using INCA-P within the framework of an automated parameter estimation
502 procedure, as was done here, is likely a reasonable approach to estimate this uncertainty³⁴.

503 MyLake's underlying conceptual model is purposely simple, in order to allow fast use of
504 the model in automated auto-calibration schemes, as was done here, or in global sensitivity
505 analysis. The drawback is that MyLake lacks the representation of some key processes, the
506 most relevant of which are identified below. First, MyLake does not represent the
507 phytoplankton community dynamic, thus not capturing possible community shifts due to
508 climate change⁵⁵. Second, MyLake does not capture the thermodynamic decrease of oxygen
509 availability at higher temperatures which, combined with the higher metabolism of respiring
510 heterotrophic organisms, enhances the risk of oxygen depletion, and ultimately of anoxia, in
511 the hypolimnion⁵. Given that hypolimnetic oxygen concentration may control P
512 sequestration and release by sediments, neglecting it introduces a source of uncertainty in
513 the model's predictions, especially for lakes with high internal P loads. As suggested by
514 Mooij et al.⁵⁶ and others^{5, 48, 57-60}, describing the exchange of phosphorus between the
515 sediments and the overlying water column beyond the daily timescale, as it is currently done
516 in MyLake, is an important step in predicting eutrophication. Although recent lake models
517 do represent internal P loading processes^{61, 62} we elected to use the simpler MyLake model
518 based on available information on internal P loading in lake Vansjø (See section 2.3). Third,
519 MyLake, as with most lake system models used to study eutrophication, does not consider
520 the coupled biogeochemical cycles of key macronutrients such as sulphur (S), calcium (Ca)
521 and iron (Fe). It has long been recognized that these elements play a key role in controlling
522 P cycling in the water column and in the sediments^{63, 64}. In oligotrophic lakes a decrease in
523 Ca concentrations, correlated with acid deposition, has been reported in Nordic lakes over
524 the past decade and may have induced changes in plankton assemblages⁶³. Finally, recent
525 increase in dissolved organic carbon (DOC) loadings to Nordic lakes⁶⁵ may have an effect
526 on the lake photon budget and thus on phytoplankton growth. Although photon absorption
527 by DOC is included in MyLake, it was not systematically investigated here due to the lack
528 of DOC data in the river. These phenomenon, acting in conjunction with climate and land-
529 use change, may be changing lakes productivity in directions that, to our knowledge, current
530 models do not predict.

531

532 **4. Conclusion**

533 This study demonstrates the usefulness and potential limitations of a novel network
534 of process-based, mass-balance models linking climate, hydrology, catchment-scale P
535 dynamics, and lake processes to support the decision-making needed to improve surface
536 water quality. The management scenarios tested here are projected to have a profound effect
537 on water quality. The model results suggest that achievement of the water quality target of
538 good ecological status in eutrophic Nordic lakes such as Lake Vansjø represents a challenge
539 given the current land use and the expected changes in climatic conditions. In order to reach
540 good water quality status, managerial choices consistent with a water-quality focus scenario
541 are needed. Such measures are deemed “climate-proof” because they will not only improve
542 water quality but also counteract the detrimental impact of projected climate change.
543 Nevertheless, consistent with previous catchment-scale studies conducted in northern³⁵,
544 central⁶⁶, and southern Europe⁶⁷, climate changes will probably worsen water quality.
545 Should the future Nordic climate (2030-2060) be wetter and warmer than that projected by
546 the A1B scenario, additional stringent management measures must be implemented in order
547 to achieve water quality. The conclusions presented here on the changes of water quality as
548 a result of management and climate change are likely to hold even if different calibration
549 periods, parameter sets, or even different catchment and lake models were used.

550 **Acknowledgments**

551 This study was funded by REFRESH (EU FP7 no. 244121), by the Strategic Institute
552 Initiative “Climate effects from Mountains to Fjords” (Research Council of Norway no.
553 208279) at NIVA and by Eutropia (Research Council of Norway no 190028/S30) at the
554 University of Oslo. Monitoring data for this study came from NIVA, NVE, Bioforsk and
555 Met.no. Monitoring programs were financed in part by MORSA. We thank stakeholders and
556 water managers at MORSA for work with the storylines. We acknowledge J.R. Selvik, A.B.
557 Christiansen, S. Haande, and A. L. Solheim (NIVA) for assistance with GIS, hydrological
558 modelling, retrieval of observation data and for discussions on the scenarios, respectively.
559

REFERENCES

- 560
561
- 562 1. D. Tilman, J. Fargione, B. Wolff, C. D'Antonio, A. Dobson, R. Howarth, D.
563 Schindler, W. H. Schlesinger, D. Simberloff and D. Swackhamer, *Science*, 2001,
564 **292**, 281-284.
 - 565 2. P. M. Haygarth, A. Delgado, W. J. Chardon, M. I. Litaor, F. Gil-Sotres and J.
566 Torrent, *Soil Use Manage.*, 2013, **29**, 1-5.
 - 567 3. V. H. Smith and D. W. Schindler, *Trends Ecol. Evol.*, 2009, **24**, 201-207.
 - 568 4. WFD, *CIS Guidance Document No. 3: Analysis of Pressures and Impacts*. 92-894-
569 5123-8, Directorate General Environment of the European Commission, Brussels,
570 2002.
 - 571 5. E. Jeppesen, B. Kronvang, M. Meerhoff, M. Sondergaard, K. M. Hansen, H. E.
572 Andersen, T. L. Lauridsen, L. Liboriussen, M. Beklioglu, A. Ozen and J. E. Olesen,
573 *J. Environ. Qual.*, 2009, **38**, 1930-1941.
 - 574 6. S. Kosten, V. L. M. Huszar, E. Becares, L. S. Costa, E. van Donk, L. A. Hansson, E.
575 Jeppesen, C. Kruk, G. Lacerot, N. Mazzeo, L. De Meester, B. Moss, M. Lurling, T.
576 Noges, S. Romo and M. Scheffer, *Glob. Change Biol.*, 2012, **18**, 118-126.
 - 577 7. J. Crossman, M. N. Futter, S. K. Oni, P. G. Whitehead, L. Jin, D. Butterfield, H. M.
578 Baulch and P. J. Dillon, *J. Gt. Lakes Res.*, 2013, **39**, 19-32.
 - 579 8. A. M. Michalak, E. J. Anderson, D. Beletsky, S. Boland, N. S. Bosch, T. B.
580 Bridgeman, J. D. Chaffin, K. Cho, R. Confesor, I. Daloglu, J. V. DePinto, M. A.
581 Evans, G. L. Fahnenstiel, L. L. He, J. C. Ho, L. Jenkins, T. H. Johengen, K. C. Kuo,
582 E. LaPorte, X. J. Liu, M. R. McWilliams, M. R. Moore, D. J. Posselt, R. P. Richards,
583 D. Scavia, A. L. Steiner, E. Verhamme, D. M. Wright and M. A. Zagorski, *P. Natl.*
584 *Acad. Sci. U.S.A.*, 2013, **110**, 6448-6452.
 - 585 9. B. Bajželj, J. M. Allwood and J. M. Cullen, *Environ. Sci. Technol.*, 2013.
 - 586 10. L. Norton, J. A. Elliott, S. C. Maberly and L. May, *Environ. Modell. Softw.*, 2012,
587 **36**, 64-75.
 - 588 11. P. G. Whitehead, L. Jin, H. M. Baulch, D. A. Butterfield, S. K. Oni, P. J. Dillon, M.
589 Futter, A. J. Wade, R. North, E. M. O'Connor and H. P. Jarvie, *Sci. Tot. Environ.*,
590 2011, **412**, 315-323.
 - 591 12. H. M. Baulch, M. N. Futter, L. Jin, P. G. Whitehead, D. T. Woods, P. J. Dillon, D. A.
592 Butterfield, S. K. Oni, L. P. Aspden, E. M. O'Connor and J. Crossman, *Inland*
593 *Waters*, 2013, **3**, 187-206.
 - 594 13. L. Jin, P. G. Whitehead, H. M. Baulch, P. J. Dillon, D. Butterfield, S. K. Oni, M. N.
595 Futter, J. Crossman and E. M. O'Connor, *Inland Waters*, 2013, **3**, 207-220.
 - 596 14. M. N. Futter, M. A. Erlandsson, D. Butterfield, P. G. Whitehead, S. K. Oni and A. J.
597 Wade, *Hydrol. Earth Syst. Sci. Discuss.*, 2013, **10**, 8635-8681.
 - 598 15. A. J. Wade, P. G. Whitehead and D. Butterfield, *Hydrol. Earth Syst. Sci.*, 2002, **6**,
599 583-606.
 - 600 16. T. M. Saloranta and T. Andersen, *Ecol. Model.*, 2007, **207**, 45-60.
 - 601 17. Ø. Kaste, R. F. Wright, L. J. Barkved, B. Bjerkeng, T. Engen-Skaugen, J.
602 Magnusson and N. R. Sælthun, *Sci. Tot. Environ.*, 2006, **365**, 200-222.
 - 603 18. A. Voinov and H. H. Shugart, *Environ. Modell. Softw.*, 2013, **39**, 149-158.
 - 604 19. F. Bouraoui, B. Grizzetti, G. Adelskold, H. Behrendt, I. de Miguel, M. Silgram, S.
605 Gomez, K. Granlund, L. Hoffmann, B. Kronvang, S. Kvaerno, A. Lazar, M.
606 Mimikou, G. Passarella, P. Panagos, H. Reisser, B. Schwarzl, C. Siderius, A. S.
607 Sileika, A. A. M. F. R. Smit, R. Sugrue, M. VanLiedekerke and J. Zaloudik, *J.*
608 *Environ. Monit.*, 2009, **11**, 515-525.

- 609 20. E. Skarbøvik and M. E. Bechmann, *Some Characteristics of the Vansjø-Hobøl*
610 *(Morsa) Catchment*, Bioforsk Soil and Environment, Ås, 2010.
- 611 21. A. Lyche Solheim, N. Vagstad, P. Kraft, Ø. Løvstad, S. Skoglund, S. Turtumøygard
612 and J. R. Selvik, *Tiltaksanalyse for Morsa (Vansjø-Hobøl-vassdraget) – Sluttrapport*
613 *OR-4377*, Norsk institutt for vannforskning (NIVA), 2001.
- 614 22. E. Skarbøvik, M. Bechmann, T. Rohrlak and S. Haande, *Overvåking Vansjø/Morsa*
615 *2008. Resultater fra overvåkingen i perioden oktober 2007 til oktober 2008* Bioforsk
616 Vol. 4, Nr 13, Bioforsk, Ås, 2009.
- 617 23. S. Haande, A. Lyche Solheim, J. Moe and R. Brænden, *Klassifisering av økologist*
618 *tilstant i elver og innsjøer i Vannområde Morsa iht. Vanndirectivet 6166-2011*,
619 Norsk institutt for vannforskning (NIVA), 2011.
- 620 24. A. M. Dolman, J. Rücker, F. R. Pick, J. Fastner, T. Rohrlack, U. Mischke and C.
621 Wiedner, *PLoS One*, 2012, **7**, e38757.
- 622 25. C. S. Reynolds, A. E. Irish and J. A. Elliott, *Ecol. Model.*, 2001, **140**, 271-291.
- 623 26. E. J. Forland, T. E. Skaugen, R. E. Benestad, I. Hanssen-Bauer and O. E. Tveito, *Art.*
624 *Antart. Alp. Res.*, 2004, **36**, 347-356.
- 625 27. N. Nakicenovic, J. Alcamo, G. Davis, B. de Vries, J. Fenhann, S. Gaffin, K.
626 Gregory, A. Grubler, T. Y. Jung, T. Kram, E. L. La Rovere, L. Michaelis, S. Mori, T.
627 Morita, W. Pepper, H. Pitcher, L. Price, K. Riahi, A. Roehrl, H.-H. Rogner, A.
628 Sankovski, M. Schlesinger, P. Shukla, S. Smith, R. Swart, S. van Rooijen, N. Victor
629 and Z. Dadi, *IPCC Special Report on Emissions Scenarios.*, Cambridge, United
630 Kingdom and New York, NY, USA, 2000.
- 631 28. C. Gordon, C. Cooper, C. A. Senior, H. Banks, J. M. Gregory, T. C. Johns, J. F. B.
632 Mitchell and R. A. Wood, *Climate Dynamics*, 2000, **16**, 147-168.
- 633 29. J. H. Jungclaus, N. Keenlyside, M. Botzet, H. Haak, J. J. Luo, M. Latif, J. Marotzke,
634 U. Mikolajewicz and E. Roeckner, *Journal of Climate*, 2006, **19**, 3952-3972.
- 635 30. T. Furevik, M. Bentsen, H. Drange, I. K. T. Kindem, N. G. Kvamstø and A.
636 Sorteberg, *Climate Dynamics*, 2003, **21**, 27-51.
- 637 31. O. H. Otterå, M. Bentsen, I. Bethke and N. G. Kvamstø, *Geosci. Model Dev.*, 2009,
638 **2**, 197-212.
- 639 32. Z. Yu, E. J. Barron and F. W. Schwartz, *Geophys. Res. Lett.*, 2000, **27**, 2561-2564.
- 640 33. N. R. Sælthun, *The "Nordic" HBV model. Description and documentation of the*
641 *model version developed for the project Climate Change and Energy Production.*,
642 Norwegian Water Resources and Energy Administration, Oslo, 1996.
- 643 34. S. Dean, J. Freer, K. Beven, A. J. Wade and D. Butterfield, *Stoch. Environ. Res. Risk*
644 *Assess.*, 2009, **23**, 991-1010.
- 645 35. C. Farkas, S. Beldring, M. Bechmann and J. Deelstra, *Soil Use Manag.*, 2013, **29**,
646 124-137.
- 647 36. Y. Dibike, T. Prowse, B. Bonsal, L. d. Rham and T. Saloranta, *Int. J. Climatol.*,
648 2012, **32**, 695-709.
- 649 37. S. Gebre, T. Boissy and K. Alfredsen, *The Cryosphere Discuss.*, 2013, **7**, 743-788.
- 650 38. E. Skarbøvik, S. Haande and M. Bechmann, *Overvåking Vansjø/Morsa 2011-2012.*
651 *Resultater fra overvåkingen i perioden oktober 2011 til oktober 2012* Bioforsk Vol.
652 **8**, Nr 71, Bioforsk, Ås, 2013.
- 653 39. J. H. Christensen, M. Rummukainen and G. Lenderink, in *ENSEMBLES: Climate*
654 *Change and its Impacts*, eds. P. van der Linden and J. F. B. Mitchell, Met Office
655 Hadley Centre, FitzRoy Road, Exeter EX1 3PB, UK, Editon edn., 2009, p. 160p.
- 656 40. M. R. Haylock, N. Hofstra, A. M. G. Klein Tank, E. J. Klok, P. D. Jones and M.
657 New, *J. Geophys. Res.-Atmosphere*, 2008, **113**, D20119.

- 658 41. M. Shahgedanova, *Down-scaled climate projections for eight demonstration*
659 *catchments under different SRES scenarios* REFRESH Deliverable 1.6, University of
660 Reading, United Kingdom, 2011.
- 661 42. J. A. Vrugt, C. J. F. ter Braak, C. G. H. Diks, B. A. Robinson, J. M. Hyman and D.
662 Higdon, *Int. J. Nonlinear Sci. Numer. Simul.*, 2009, **10**, 273-290.
- 663 43. K. Tominaga, University of Oslo, 2013.
- 664 44. D. N. Moriasi, J. G. Arnold, M. W. Van Liew, R. L. Bingner, R. D. Harmel and T. L.
665 Veith, *T. ASABE*, 2007, **50**, 885-900.
- 666 45. F. J. Los and M. Blaas, *J. Marine Syst.*, 2010, **81**, 44-74.
- 667 46. J. K. Jolliff, J. C. Kindle, I. Shulman, B. Penta, M. A. M. Friedrichs, R. Helber and
668 R. A. Arnone, *J. Marine Syst.*, 2009, **76**, 64-82.
- 669 47. I. Panagopoulos, M. Mimikou and M. Kapetanaki, *J Soils Sediments*, 2007, **7**, 223-
670 231.
- 671 48. M. Sondergaard, R. Bjerring and E. Jeppesen, *Hydrobiologia*, 2013, **710**, 95-107.
- 672 49. *The impact of climate change on European lakes*, Dordrecht : Springer, c2010, 2010.
- 673 50. M. Vetter and A. Sousa, *Fundam. Appl. Limnol.*, 2012, **180**, 41-57.
- 674 51. A. Iversen, *Klassifisering av miljøtilstand i vann Økologisk og kjemisk*
675 *klassifiseringssystem for kystvann, innsjøer og elver i henhold til vannforskriften*,
676 Direktoratgruppen for gjennomføringen av vanndirektivet, Trondheim, Norway,
677 2009.
- 678 52. S. J. Moe, in *Environmental Risk Assessment and Management from a Landscape*
679 *Perspective*, eds. L. Kapustka, W. G. Landis and A. Johnson, Wiley's, Hoboken,
680 New-Jersey, Editon edn., 2010, p. 396p.
- 681 53. D. Karssenberg, O. Schmitz, P. Salamon, K. de Jong and M. F. P. Bierkens, *Environ.*
682 *Modell. Softw.*, 2010, **25**, 489-502.
- 683 54. T. J. Coulthard, M. J. Kirkby and M. G. Macklin, *Hydrol. Process.*, 2000, **14**, 2031-
684 2045.
- 685 55. C. C. Carey, B. W. Ibelings, E. P. Hoffmann, D. P. Hamilton and J. D. Brookes,
686 *Water Research*, 2012, **46**, 1394-1407.
- 687 56. W. Mooij, D. Trolle, E. Jeppesen, G. Arhonditsis, P. Belolipetsky, D. Chitamwebwa,
688 A. Degermendzhy, D. DeAngelis, L. De Senerpont Domis, A. Downing, J. Elliott, C.
689 Fragoso, U. Gaedke, S. Genova, R. Gulati, L. Håkanson, D. Hamilton, M. Hipsey, J.
690 't Hoen, S. Hülsmann, F. Los, V. Makler-Pick, T. Petzoldt, I. Prokopkin, K. Rinke,
691 S. Schep, K. Tominaga, A. Van Dam, E. Van Nes, S. Wells and J. Janse, *Aquatic*
692 *Ecology*, 2010, **44**, 633-667.
- 693 57. M. Sondergaard, J. P. Jensen and E. Jeppesen, *Freshw. Biol.*, 2005, **50**, 1605-1615.
- 694 58. S. Katsev and M. Dittrich, *Ecol. Model.*, 2013, **251**, 246-259.
- 695 59. G. K. Nürnberg, L. A. Molot, E. O'Connor, H. Jarjanazi, J. Winter and J. Young, *J.*
696 *Gt. Lakes Res.*, 2013, **39**, 259-270.
- 697 60. J. McCulloch, A. Gudimov, G. Arhonditsis, A. Chesnyuk and M. Dittrich, *Chemical*
698 *Geology*, 2013, **354**, 216-232.
- 699 61. D. F. Burger, D. P. Hamilton and C. A. Pilditch, *Ecol. Model.*, 2008, **211**, 411-423.
- 700 62. J. G. C. Smits and J. K. L. van Beek, *PLoS One*, 2013, **8**.
- 701 63. K. Hadley, A. Paterson, R. Hall and J. Smol, *Aquat. Sci.*, 2013, **75**, 349-360.
- 702 64. J. Lehtoranta, P. Ekholm and H. Pitkanen, *Ambio*, 2009, **38**, 303-308.
- 703 65. G. B. Lawrence, J. E. Dukett, N. Houck, P. Snyder and S. Capone, *Environ. Sci.*
704 *Technol.*, 2013, **47**, 7095-7100.
- 705 66. J. Kopáček, J. Hejzlar and M. Posch, *Biogeochemistry*, 2013, **115**, 1-17.
- 706 67. F. Caille, J. L. Riera and A. Rosell-Melé, *Hydrol. Earth Syst. Sci.*, 2012, **16**, 2417-
707 2435.

708 68. J. Starrfelt and Ø. Kaste, *Environ. Sci.: Processes Impacts*, 2014, DOI:
 709 10.1039/C3EM00619K
 710

711 **Tables**

712 **Table 1.** Location and characteristics of the lake basins.

Basin name	Storefjorden	Vanemfjorden
Location (Lat, Lon)	59°23'24'' N, 10°49'52''E	59°24'53'' N, 10°42'46'' E
Mean depth (m)	8.7	3.8
Maximum depth (m)	41.0	19.0
Area (km ²)	23.8	12
Volume (m ³)	206.1×10 ⁶	46.1×10 ⁶
Residence time (yr)	0.85	0.21

713

714 **Table 2.** Change in yearly mean temperature (ΔT) and precipitation (Δp) predicted by
 715 climate models for the Vansjø-Hobøl catchment during the scenario period 2030-2052
 716 relative to the reference period 1990-2012.

Scenario	GCM	RCM	ΔT ($^{\circ}\text{C}$)	Δp (mm)	Configuration
C1	HadRm3 ^a	HADRM3	+1.6	+78.8	Q0 with normal sensitivity
C2	ECHAM5 ^b	RACMO	+0.7	+43.4	-r3 set of initial conditions
C3	BCM ^c	RCA	+0.9	□10.5	

717 ^a) Hadley Centre, UK; ^b) Max Planck Institute for Meteorology, Germany; ^c) Nansen
 718 Centre, Norway

719

720 **Table 3.** Summary of models performance statistics. Coefficient of determination (R^2),
 721 Root-mean-square error (RMSE), and Nash-Sutcliffe coefficient on normal (NS) and log-
 722 transformed data (NS_{\log}) for reach R4 (Hobøl at Kure), station L1 (Storefjorden) and L2
 723 (Vanemfjorden) of the model network.

Parameter	Model (Station)	R^2	RMSE	NS	NS_{\log}
Q	PERSiST (R4)	0.85	52.58 $\text{m}^3 \text{s}^{-1}$	0.85	0.99
Q	INCA-P (R4)	0.59	3.34 $\text{m}^3 \text{s}^{-1}$	0.48	0.99
TP	INCA-P (R4)	0.04	0.09 $\mu\text{g L}^{-1}$	-0.51	0.16
TP	MyLake (L1)	0.93	6.37 $\mu\text{g L}^{-1}$	0.19	0.99
TP	MyLake (L2)	0.94	7.76 $\mu\text{g L}^{-1}$	-0.23	0.99
PO_4	MyLake (L1)	0.92	6.70 $\mu\text{g L}^{-1}$	0.39	0.84
PO_4	MyLake (L2)	0.72	2.54 $\mu\text{g L}^{-1}$	-0.96	0.90
Chl	MyLake (L1)	0.74	4.48 $\mu\text{g L}^{-1}$	-0.68	0.89
Chl	MyLake (L2)	0.82	8.11 $\mu\text{g L}^{-1}$	0.21	0.96
PP	MyLake (L1)	0.47	11.36 $\mu\text{g L}^{-1}$	-0.52	0.92
PP	MyLake (L2)	0.85	8.16 $\mu\text{g L}^{-1}$	-0.50	0.98

724

725 **Table 4.** Proportion (%) of days above the good/moderate or the moderate/bad thresholds
 726 set by the WFD for TP and Chl for basins of classes L-N3 (Storefjorden) and L-N8
 727 (Vanemfjorden) in the months of June, July and August. Lower numbers indicate better
 728 water quality.

Threshold name	Good/Moderate				Moderate/Bad			
	Storefj.		Vanemfj.		Storefj.		Vanemfj.	
Basin	TP	Chl	TP	Chl	TP	Chl	TP	Chl
Parameter	TP	Chl	TP	Chl	TP	Chl	TP	Chl
Threshold values (ug L ⁻¹)	16	7.5	19	10.5	30	35	15	20
Reference (%)	99	99	99	95	21	32	58	58
Storyline 1 (%)	92	99	88	90	0	0	30	29
Storyline 4 (%)	98	99	99	99	94	95	99	93

729

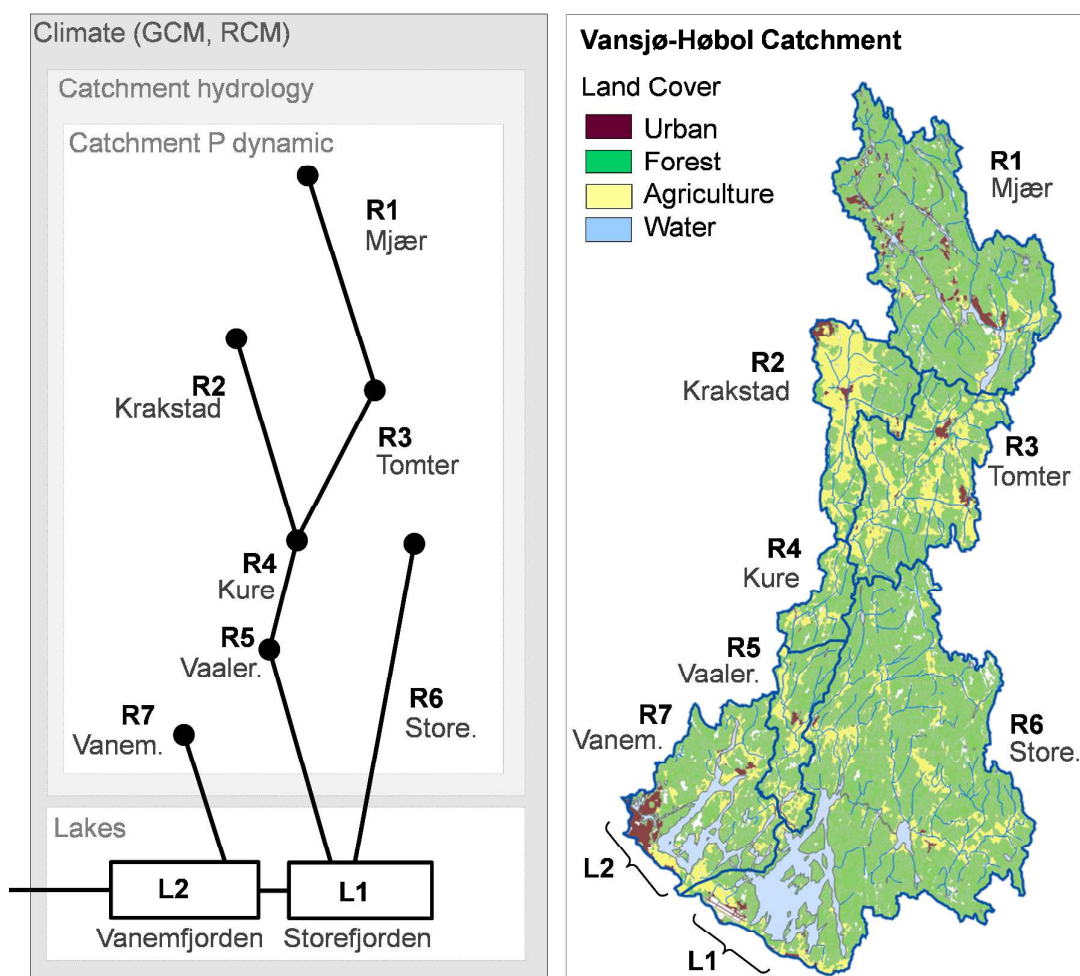
730

731

732

733 **Figures**

734



735

736

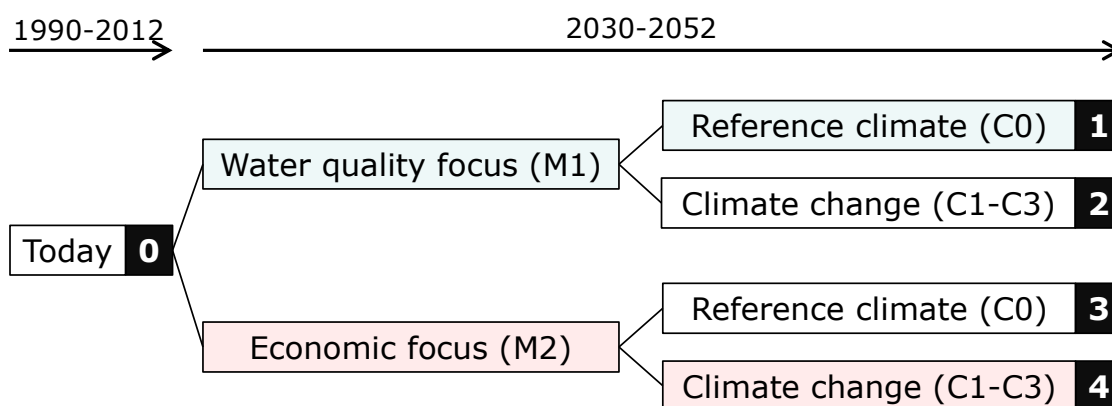
737

738

739

740

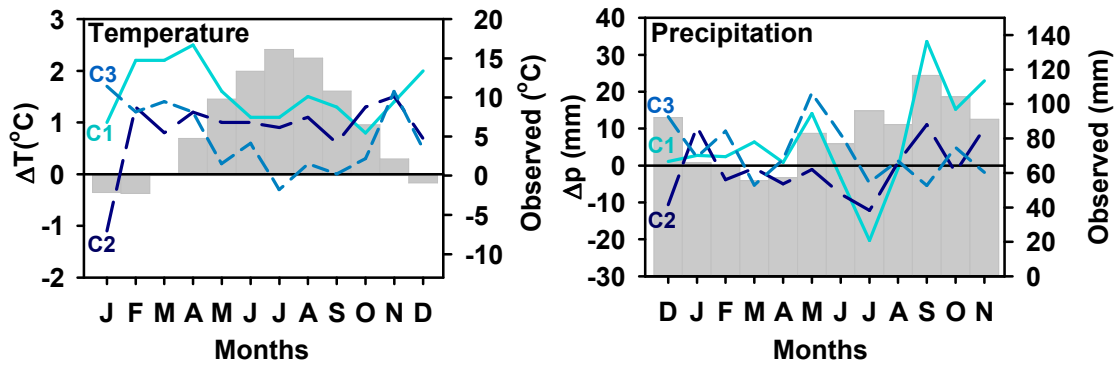
Figure 1. Land-use distribution of the Vansjø-Høbol catchment (right panel) and corresponding schematic representation of the catchment-lake model network (left panel) indicating river reaches (R) modelled with INCA-P and lake basins (L) modelled with MyLake. The hydrological model PERSiST provides input for the catchment model, and the climate models provide forcing for all models.



741
742

743 **Figure 2.** Management and climate scenarios defining the storylines. Storyline 0 represents
744 the reference management focus and reference climate that were compared to observations
745 in calibrating the river-lake model network and deriving model performance metrics.

746



747

748

749

750

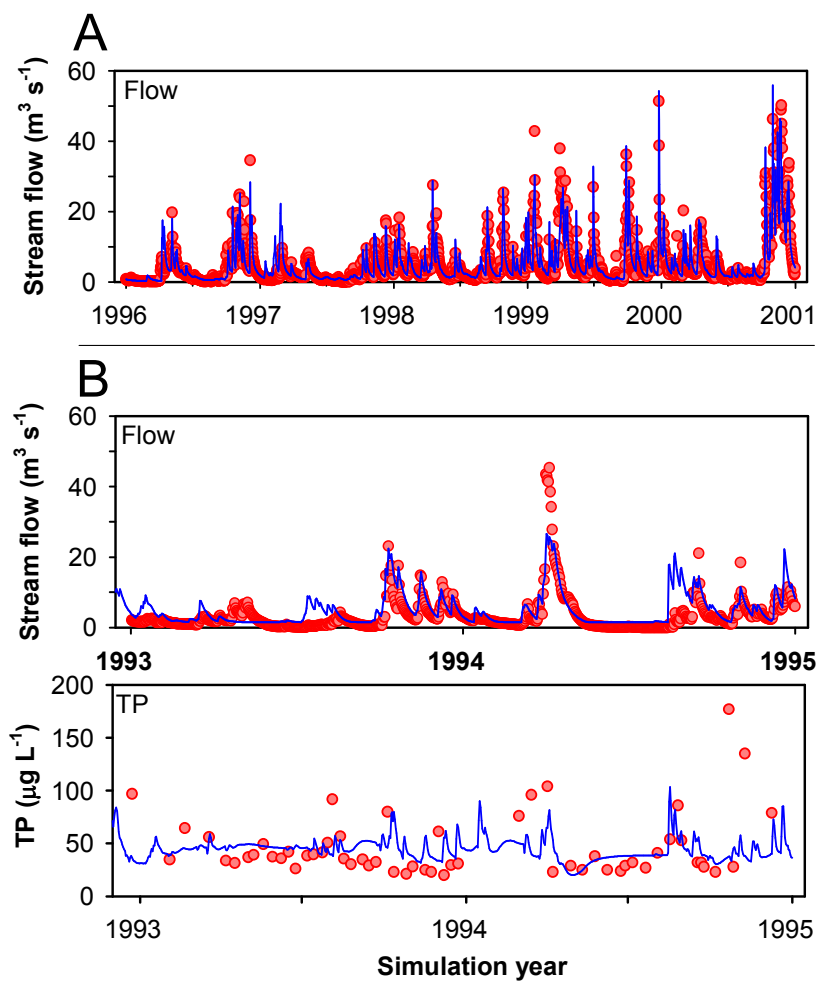
751

752

753

Figure 3. Monthly means of the changes in temperature and precipitation imposed by the climate models HadCM3/HadRM3 (solid line, C1), ECHAM5/RACMO (long dashed line, C2) and BCM/RCA (short dashed line, C3) for the period of 2030-2052 relative to the present-day conditions (C0) over the period of 1990-2012, along with monthly means of observed temperature and precipitation over the same period (grey vertical bars).

754

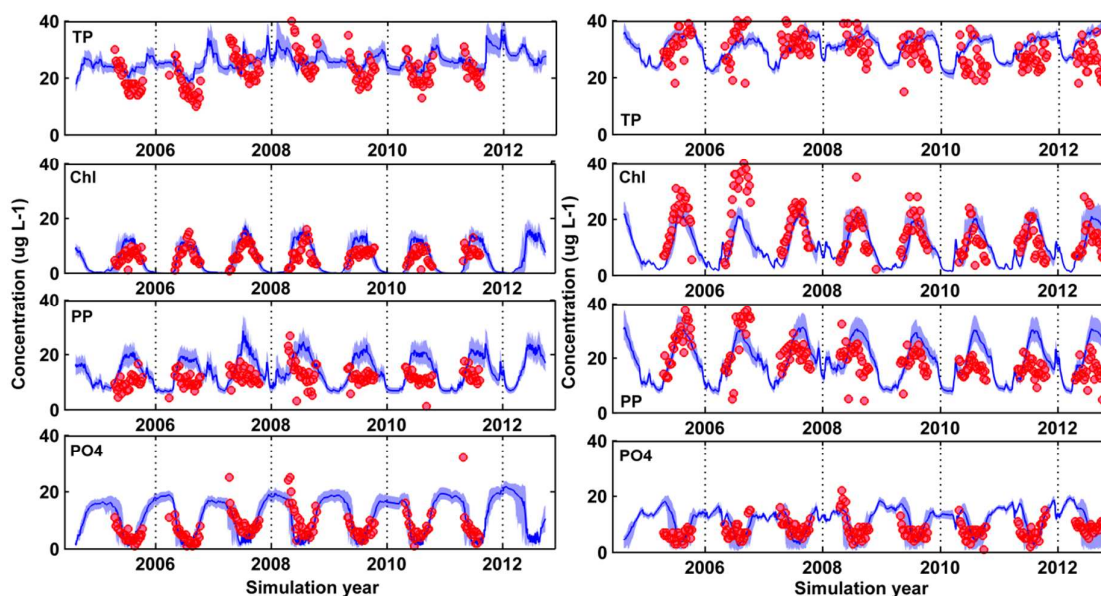


755

756

757 **Figure 4.** Observed (symbols) and simulated (solid line) stream flow at the end of R4 using
758 the model PERSiST (panel A), as well as observed and simulated stream flow and TP at the
759 end of R4 using INCA-P (panel B).

760



761

762

763

764

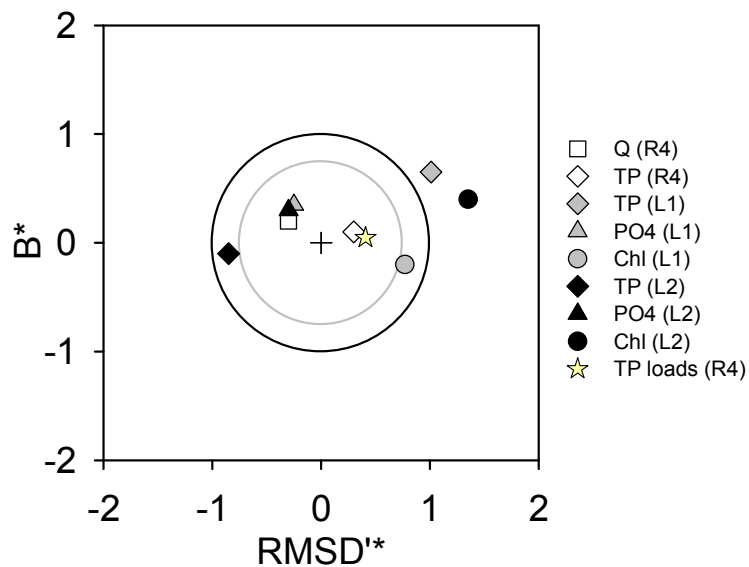
765

766

Figure 5. Calibration performance of MyLake at Storefjorden (L1, left panels) and Vanemfjorden (L2, right panels) for total phosphorus (TP), chlorophyll (Chl), particulate phosphorus (PP) and phosphate (PO₄) over the calibration period of 2005-2012. The results are reported as the median (solid line), daily quartile statistics sampled from the parameter sets of equal likelihood (continuous area) together with the observations (circles).

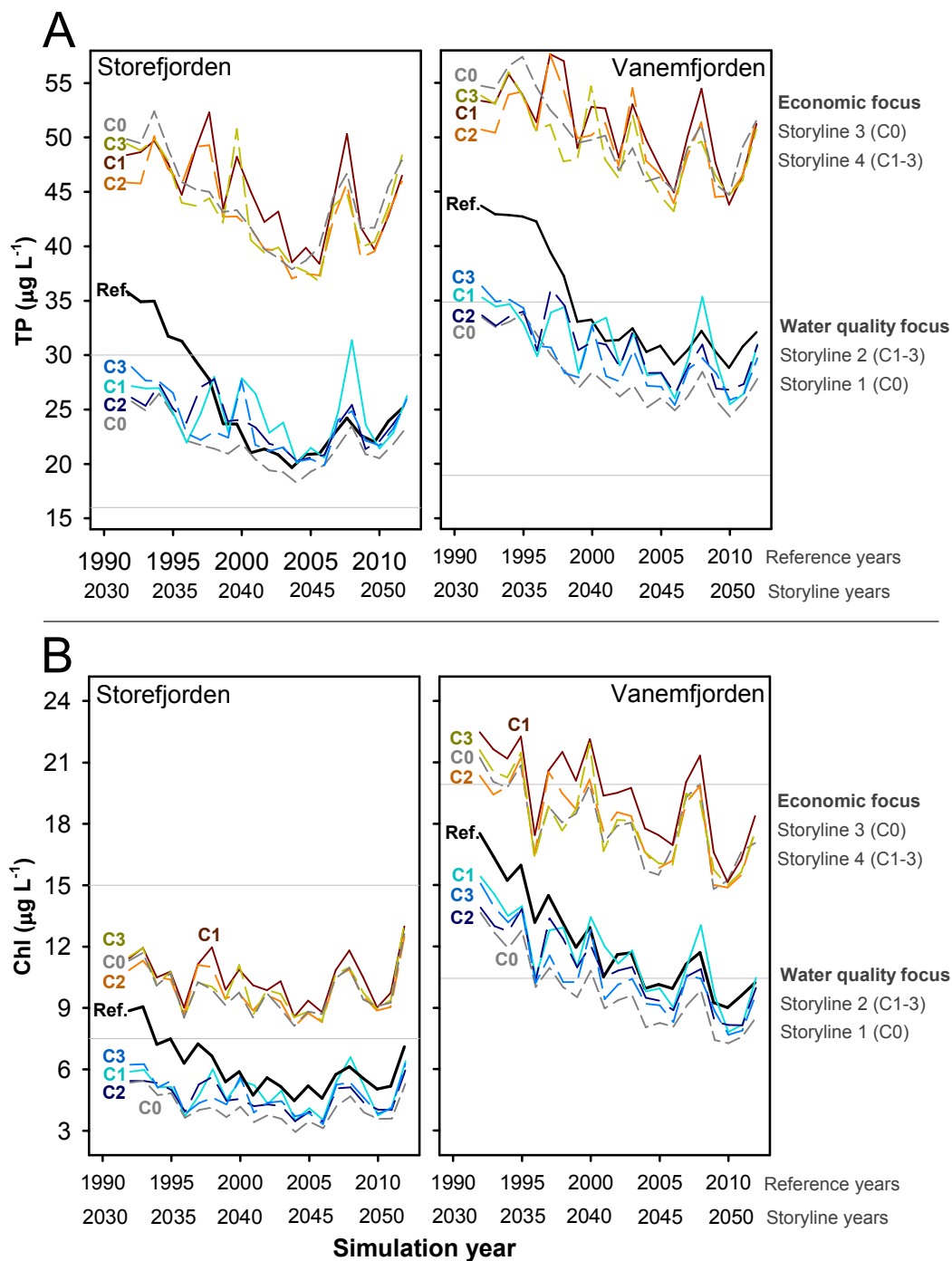
767

768



769

770 **Figure 6.** Target diagram presenting the normalized bias (B^*) against normalized unbiased
771 root mean square difference ($RMSD'^*$) of simulated Q, TP and TP loads for INCA-P at R4
772 and of simulated TP, PO_4 , and Chl for MyLake at Vanemfjorden and Storefjorden over the
773 calibration periods. The median simulated values were used for TP, PO_4 and Chl. The inner
774 and outer circles indicate ± 0.75 and ± 1 standard deviation (σ) on the X-axis and 75% and
775 100% B^* on the Y-axis, respectively.



776

777

778

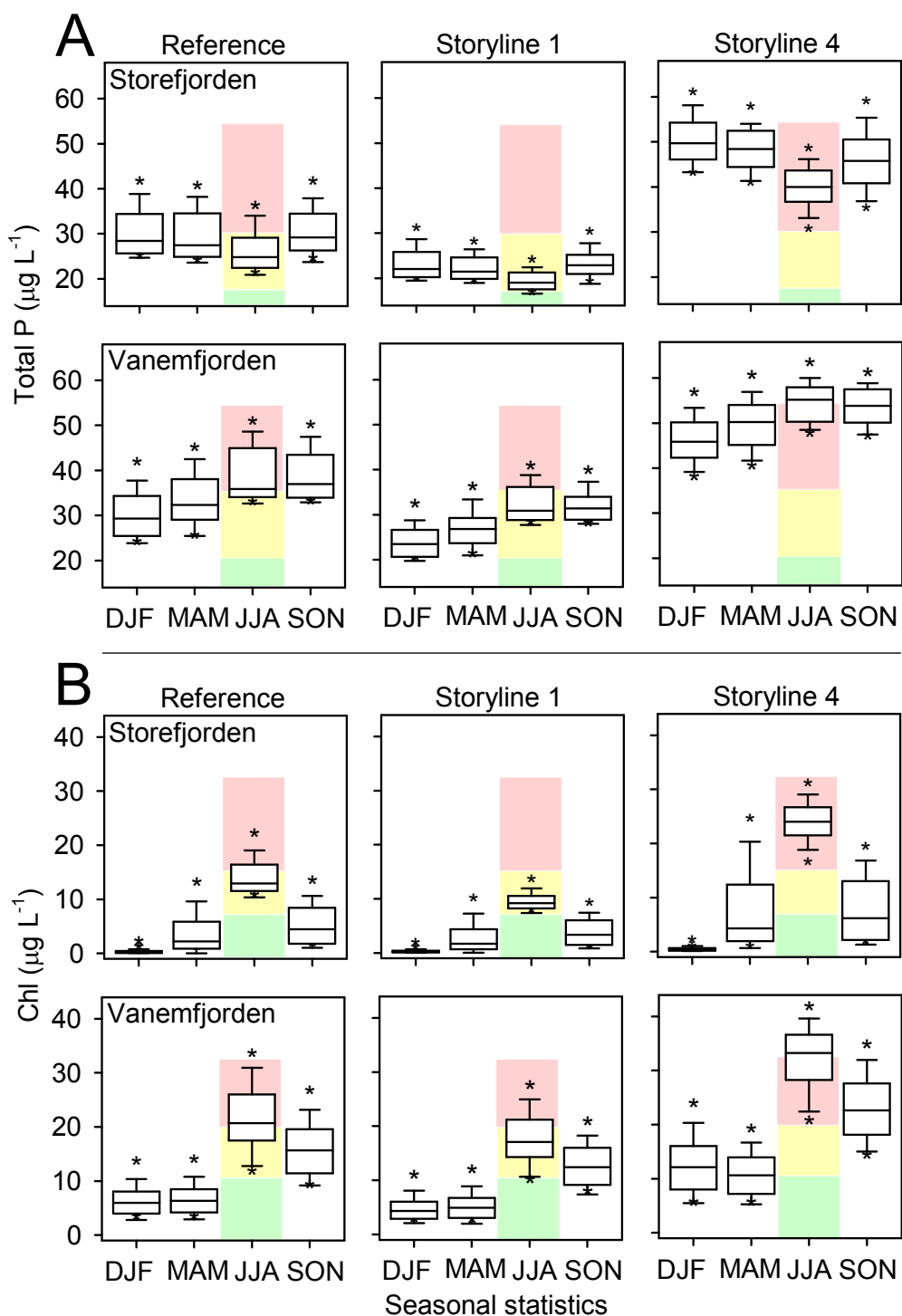
779

780

781

782

Figure 7. Predicted yearly median total P (panel A) and Chlorophyll (panel B) at Storefjorden (L1) and Vanemfjorden (L2) by the MyLake model without (C0; Storylines 1 and 3) or with climate change predictions made by the HadRm3 (C1), the ECHAM5 (C2) or the BCM models (C3) as climate forcing (Storylines 2 and 4) for the river-lake model network. The thick solid lines represent the reference conditions and the thin horizontal solid lines indicate the WFD thresholds specific to each basin (see Table 4).



783

784 **Figure 8.** Seasonal range of MyLake-predicted daily TP (panel A) and Chlorophyll (panel
 785 B) concentrations in the top 4m of the Storefjorden (L1) and Vanemfjorden (L2) water
 786 columns. The green, yellow and red shaded zones indicate the basin-specific WFD water
 787 quality targets for good, moderate and bad water quality status, respectively (see Table 4),
 788 while the asterisks indicate the 5th and 95th percentile outliers.